

Review

Dispersion of Nanoparticles in Lubricating Oil: A Critical Review

Yan Chen ¹, Peter Renner ² and Hong Liang ^{1,2,*} 

¹ Department of Materials Science and Engineering, Texas A&M University, College Station, TX 77843-3123, USA; yanchen876@tamu.edu

² J. Mike Walker '66 Department of Mechanical Engineering, Texas A&M University, College Station, TX 77843-3123, USA; parenner@tamu.edu

* Correspondence: hliang@tamu.edu

Received: 10 December 2018; Accepted: 5 January 2019; Published: 10 January 2019



Abstract: Nanolubricants have attracted great interest due to the promise of friction and wear reduction by introducing nanoparticles. To date, the foremost challenge for developing a new nanolubricant is particle suspension. To understand the mechanisms of nanoparticle dispersion and identify bottlenecks, we conducted a comprehensive review of published literature and carried out an analysis of dispersion based on available data from the past 20 years. This research has led to three findings. First, there are two primary methods in dispersion: formulation with dispersant and surface modification. Second, surfactant and alkoxy-silanes are primary chemical groups used for surface modification. Third, functionalization using surfactant is found to be suitable for nanoparticles smaller than 50 nm. For larger particles (>50 nm), alkoxy-silanes are the best. The existence of a critical size has not been previously known. To better understand these three findings, we conducted an analysis using a numerical calculation based on colloidal theory. It revealed that a minimal thickness of the grafted layer in surfactant-modified nanoparticles was responsible for suspending small nanoparticles. For larger nanoparticles (>50 nm), they were suitable for silanization of alkoxy-silane due to increased grafting density. This research provides new understanding and guidelines to disperse nanoparticle in a lubricating oil.

Keywords: nanoparticles; nanolubricants; dispersion; suspension; functionalization

1. Introduction

In mechanical systems, the frictional loss is one of many factors in energy consumption [1]. To reduce friction and wear, nanoparticles have been studied to be used as lubricant additives that have promising effects on friction and wear reduction in automotive [2,3], mining [4], and other industrial applications [5]. Nanoparticles of various compositions and sizes have demonstrated certain degrees of friction modifying and anti-wear effects. We recently reported that in the boundary lubrication region, the addition of nanoparticles can reduce the friction coefficient up to 70%, and wear volume as high as 75% [5]. Such lubricants consisting of a base oil and dispersed nanoparticles emerged as a new class of nanolubricants [5,6]. The bottleneck for further development, however, is the aggregation of nanoparticles in a base oil. A stable suspension of nanoparticles is essential for a usable lubricant. The aggregation of nanoparticles limits their ability to lubricate the contact area [7]. The MoS₂ nanoparticle can reduce 75% of friction when mixed with lubricant oil. Such reduction was achieved by ultrasonic dispersion immediately before testing [8,9]. The aggregation of nanoparticles could increase friction due to the reduced “shear” effects [9]. Understanding the principles of dispersion is essential to developing novel lubricants. This review is divided into two parts. The first part reviews the methods used to disperse nanoparticles in lubricant oil. The second studies the mechanisms of dispersion.

2. Dispersion Methods

There are many ways to characterize nanoparticles suspended in oil. As nanolubricants require a long time to become stable, methods have been reported to examine dispersion in time. The widely used method is visual inspection [10–27]. The lubricant dispersed with nanoparticles is visually different compared to a lubricant. This makes the occurrence of aggregation and the following sedimentation distinguishable through visual inspection.

One of the commonly used method is visible light scattering. The dynamic light scattering (DLC) method has been used to measure the hydrodynamic radius of nanoparticles. This method tracks the scattering of polarized light from a work piece [28] and calculates the radius of the nanoparticles. The increase of hydrodynamic radius of nanoparticles signals the occurrence of aggregation. Several studies used UV-visible spectroscopy to track the sample's light absorption. The decrease of optical absorption inferred the aggregation and sedimentation of nanoparticles [29]. A previous study reported on stabilization time of the nanoparticle dispersion in a base oil. The time to reach stable for nanoparticles is summarized in Table 1. The factors affecting suspension are particle size, medium, and methods to disperse. Results shown in Table 1 lead to the conclusion that Brownian motion and gravity could affect dispersion [30]. Ironically, the stability has been characterized in only a small quantity in most studies. Those studies, in addition, cannot be applied directly to colloidal particles [31,32]. In particular, understanding the dispersion of nanoparticles at high concentration is needed.

There are two strategies to achieve stable suspension of nanoparticles in lubricant oil. One is to change the formulation of the lubricating oil by incorporating dispersant with nanoparticles. The other is to modify nanoparticles with amphiphilic chemicals or alkoxysilanes. Both methods alter the surface of nanoparticles by absorption or chemical reaction to form an organic layer.

Table 1. The publications researched in this review.

Particle	Size (nm)	Media	Disperse Method *	Stability	Stable Time
Oxides					
TiO ₂	2	liquid paraffin	SSM.	stable	1 month [10]
	5	liquid paraffin	SSM.	not reported	[33]
	10	liquid paraffin	SSM.	stable	Claimed [34]
	15	PAO Spectrasyn 4	SI-ATRP	stable	56 days [11]
	23	PAO	None	aggregated	[35]
	25	liquid paraffin	Silanization + Dispersant	stable	5 months [12]
	75	AOI group III	None	not reported	[36]
SiO ₂	12	PAO	NIM	stable	2 days [13]
	15	Ionic liquid	None	aggregated	[37]
	23	PAO Spectrasyn 4	SI-ATRP	stable	56 days [11]
	23	PAO	SI-ATRP	stable	60 days [14,38]
	25	GMO	Silanization	stable	5 months [39]
	45	EOT5	None	not reported	[15]
	60	PAO 100	Silanization	stable	2 months [16]
	100	RO base oil	Silanization	stable	8 days [17]
	110	PAO	Silanization	stable	2 months [40]
	200	PAO	Silanization	stable	4 months [18]
	200	PAO	Silanization	stable	2 months [41]
ZrO ₂ /SiO ₂	100	20# machine oil	Other	stable	12 h [42]
Al ₂ O ₃ /SiO ₂	70	liquid paraffin	Silanization	stable	3 months [19]
CuO	5	PAO	SSM.	stable	30 days [43]
	40	PAO 6	None	not reported	[44]
ZnO/CuO	40	vegetable oil	None	not reported	[45]
ZrO ₂	25	PAO 6	None	not reported	[44]
ZnO	20	PAO 6	None	not reported	[44]
ZnO/Al ₂ O ₃	50	20# machine oil	SSM.	stable	28 days [20]
Fe ₃ O ₄	10	liquid paraffin	SSM.	stable	Claimed [46]
Fe ₂ O ₃	30	500 SN basic oil	Dispersant	Stable	Claimed [47]
Al ₂ O ₃	80	20# machine oil	SSM.	stable	20 days [21]
Al ₂ O ₃ /TiO ₂	100	base oil	Silanization	stable	110 h [48]
GO/ZrO ₂	5	liquid paraffin	Other	stable	48 h [22]

Table 1. Cont.

Particle	Size (nm)	Media	Disperse Method *	Stability	Stable Time
Sulfide					
PbS	5	liquid paraffin	SSM.	stable	Claimed [49]
IF-WS ₂	65	PAO	None	not reported	[50]
	100	PAO	None	stable	hours [51]
	110	liquid paraffin	Silanization	stable	14 days [23]
WS ₂	120	liquid paraffin	None	aggregated	[52]
	7	PAO	SSM.	stable	6 months [24]
	100	liquid paraffin	SSM.	stable	Claimed [25]
IF-MoS ₂	200	liquid paraffin	SSM.	stable	1 day [53]
	35	PAO/Hexane	None	not reported	[54]
MoS ₂	3	PAG	SSM.	stable	2 weeks [55]
	15	250X base oil	Dispersant	stable	Claimed [56]
	85	EOT5	None	not reported	[15]
MoS ₂ sheets	90	coconut/paraffin oil	SSM.	stable	2 days [57]
	N/A	PAO	SSM.	stable	7 days [58]
Mo ₁₅ S ₁₉	10	Linseed Oil	None	not reported	[59]
MoS ₂ /TiO ₂	125	rapeseed oil	None	stable	2 days [26]
CuS	20	liquid paraffin	SSM.	stable	Claimed [60]
Metal					
Cu	5	liquid paraffin	SSM.	stable	months [10]
	9	500SN base oil	SSM.	stable	Claimed [61]
	15	liquid paraffin	SSM.	stable	Claimed [62]
	40	raw oil	Dispersant	not reported	[63]
	75	500SN base oil	Dispersant	aggregated	[64]
Carbon-coated Cu	65	PAO6	None	not reported	[65]
Mo	60	PEG	None	not reported	[66]
Ni	8	PAO	SSM.	stable	1 month [67]
	20	500SN base oil	Dispersant	stable	Claimed [68]
	20	PAO	None	stable	hours [69]
Ag	4	liquid paraffin	SSM.	stable	months [10]
	4	PAO	SSM.	stable	3 months [70]
	6	PEG	SSM.	stable	7 months [71]
	6	Kerosene	SSM.	stable	months [72]
	10	liquid paraffin	SSM.	not reported	[73]
Pd	15	liquid paraffin	SSM.	stable	7 days [74]
	2	liquid paraffin	SSM.	stable	Claimed [75]
	2	liquid paraffin	SSM.	not reported	[76]
Pb	3	PAO	SSM.	stable	months [77]
	40	liquid paraffin	SSM.	stable	claimed [78]
Carbon					
Graphene	N/A	liquid paraffin	Dispersant	not reported	[79]
	N/A	SAE 10W30	None	not reported	[80]
	N/A	PAO 9	SSM.	stable	Claimed [81]
	N/A	SN350	SSM.	stable	6 h [29]
	N/A	hexadecane	SSM.	stable	2 days [82]
	N/A	PEG400	NIM	stable	30 days [83]
Graphene Oxide	N/A	mineral oil	Dispersant	not reported	[84]
	N/A	SAE 5W30	None	not reported	[85]
	N/A	PAO	None	not reported	[86]
Carbon Spheres	200	SAE 5W30	None	not reported	[87]
Nanodiamond	5	paraffin	None	not reported	[88]
	10	paraffin	SSM	not reported	[89]
	30	Diisodecyl Adipate	None	not reported	[90]
Fullerene	10	ISO68 base oil	None	not reported	[91]
	10	mineral oil	None	not reported	[92]
Carbon nano-onions	4	PAO	None	aggregated	[93]
	10	PAO	None	not reported	[94]
	5	PAO	None	not reported	[95]
Carbon nano-horns	97	Mobil Pegasus 1005	Dispersant	stable	14 days [27]
Carbon nanotube	100	PAO	Dispersant	stable	24 h [96]
	N/A	lubricant oil	Dispersant	not reported	[97]
	N/A	liquid paraffin	None	not reported	[98]
	N/A	sunflower oil	Dispersant	not reported	[99]
	N/A	ionic liquid	None	stable	Claimed [100]
	N/A	rapeseed oil	SSM	stable	10 days [101]

Table 1. Cont.

Particle	Size (nm)	Media	Disperse Method *	Stability	Stable Time
Other					
CaCO ₃	20	500SN base oil	Dispersant	not reported [102]	
	40	PAO	SSM.	stable	Claimed [103]
	45	dodecane /decane	Dispersant	stable	Claimed [104]
Zinc borate	35	500 SN basic oil	Dispersant	stable	Claimed [105]
	95	Lubricant oil	SSM.	unstable [106]	
La(OH) ₃	30	liquid paraffin	None	Not reported [107]	
LaB	30	500SN base oil	Dispersant	stable	Claimed [108]
LaF ₃	6	liquid paraffin	SSM.	stable	Claimed [109]
	8	liquid paraffin	SSM.	stable	months [10]
BN	70	POE	Silanization	stable	10 days [110]

* Abbreviations: SSM: Surfactant/organic surface modification. NIM: Nanoscale ionic materials. SI-ATRP: Surface-induced atomic transfer radical polymerization.

The property of nanoparticles, the dispersion method, and resulting suspension are listed in Table 1. The stable time was retrieved from either visual inspection or light scattering results. Each time represents the duration of nanoparticles which stay dispersed in a lubricating oil without aggregation and sedimentation. If there was no stabilizing time given or no empirical proof of long-term stabilization, the stabilization time was marked as “Claimed”.

One conclusion can be immediately deduced from Table 1 that all well-dispersed nanoparticle additives are either formulated with dispersants or with surface modification. Without a proper dispersion method, the aggregation always occurs, no matter the material or shape of nanoparticles.

2.1. Formulation with Dispersant

In early research (before 2005), the common method used to study the effects of nanoparticles in lubricant was to disperse these nanoparticles using dispersants [47,56,64,68,79,102,105]. The dispersants used including Aliquat 336 [68], Estisol 242 [12], oleic acid [12], sorbitol monostearate [47,105], and several others. These dispersants were mixed with the nanoparticles and the lubricant oil to create a stable dispersion. In some cases, multiple types of dispersants were used simultaneously [12].

The mechanism of dispersant-stabilizing nanoparticles was through absorption on the surface of the nanoparticle. Those dispersants were amphiphilic molecules which had both lipophobic and lipophilic functional groups. The lipophobic part can absorb on the surface of the nanoparticle, forming an organic layer [111]. This organic layer can sterically stabilize the nanoparticles. In some cases, the addition of dispersant lowered the effectiveness of nanoparticles [112].

Among the studies where only dispersant was used, none achieved long-time stability. The stable time was either untested or less than a few weeks. The one which reached long-time stability (5 months) used a nanoparticle with silane surface modification [12].

Furthermore, the dispersion agent also changed the formulation of lubricant oil. The mechanism of dispersant-stabilizing nanoparticles was absorption on the surface of the nanoparticles. This absorption could occur on the surface of the tribological pairs where lubricant was used. In addition, the amount of dispersant added was more than the amount of nanoparticles in this method [56,68,105,108], and the property of nanolubricant was altered. In the case of IF-WS₂ nanoparticles, the addition of dispersant lowered its effectiveness [112].

Recently, the synergetic friction modification effects between ionic liquid and nanoparticle additives have been investigated [38,66,80]. It is possible that the addition of ionic liquid improves the dispersion stability of nanolubricants. One report, in particular, showed a long stable time [38].

The drawbacks mentioned above rendered formulation with dispersant an unideal method to disperse nanoparticles in lubricant oil. It was clear that surface modification methods were needed to form a stable nanoparticle dispersion.

2.2. Surface Modification

In recent years, methods of surface modification of nanoparticles as lubricant additives have shown visible improvements. Figure 1 shows the accumulated number of papers on different methods plotted against the publication year. This section discusses about methods, specifically the processes, their effectiveness and corresponding processes in achieving stable suspension.

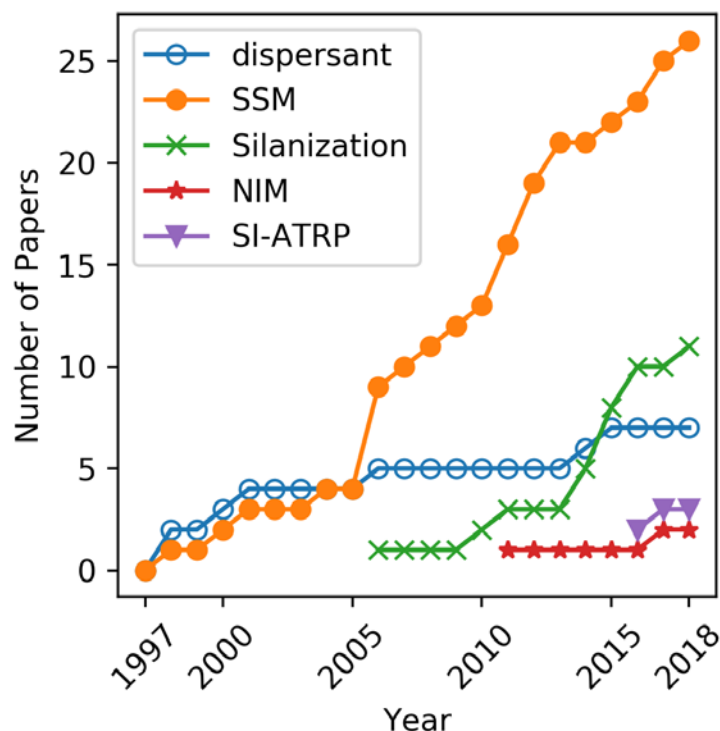


Figure 1. The accumulated number of publications using different methods each year.

2.2.1. Surfactant

Surfactant modification was one of the most widely used methods for nanoparticle dispersion (Table 1). Instead of adding surfactants to the lubricant oil as a dispersant, this method attaches surfactant molecules onto the surface of the nanoparticle. The formulation of lubricant oil was not changed to suit the need of nanoparticle dispersion.

The method of surfactant modification uses the surfactant with functional groups that can react with nanoparticle surfaces. Some examples of these surfactants are shown in Figure 2 [113]. Each of these surfactants has an active group and a long alkyl chain containing about 15 carbon atoms. These surfactants were used to directly modify nanoparticles' surfaces. This was performed by mixing nanoparticles, solvent, and surfactant at an elevated temperature for a certain amount of time. Nanoparticles need to be well dispersed in the solvent, or the surface modification process can be impeded [114]. Different nanoparticles and surfactants have different reaction mechanisms. For example, the carboxyl group in carboxylic acid can react with the hydroxyl group on the oxide nanoparticles through esterification [34,81,115,116], while cationic surfactants can ionically bond to the surface of the nanoparticles [10,53,62,67,117].

Treating the metal oxide nanoparticle surface first with acid or oxidant can enhance the binding between nanoparticles and surfactant, thus, enhancing the dispersibility of nanoparticles [114,118]. Without these treatments, some of the surfactant do not chemically bond to the surface of the nanoparticle [115,116], and can be dissolved into the lubricant oil when the solubility of the surfactant in the oil is high [116]. However, these treatments cannot effectively modify metal sulfide nanoparticles [57]. The metal sulfide nanoparticles have the best performance as a friction modifying

additive [5]. Due to the lack of the hydroxyl group, however, modifying metal sulfide nanoparticles' surfaces with amine or carboxylic acids was difficult. Therefore, the sulfide nanoparticles modified with surfactant resulted in dispersions with low stability [57].

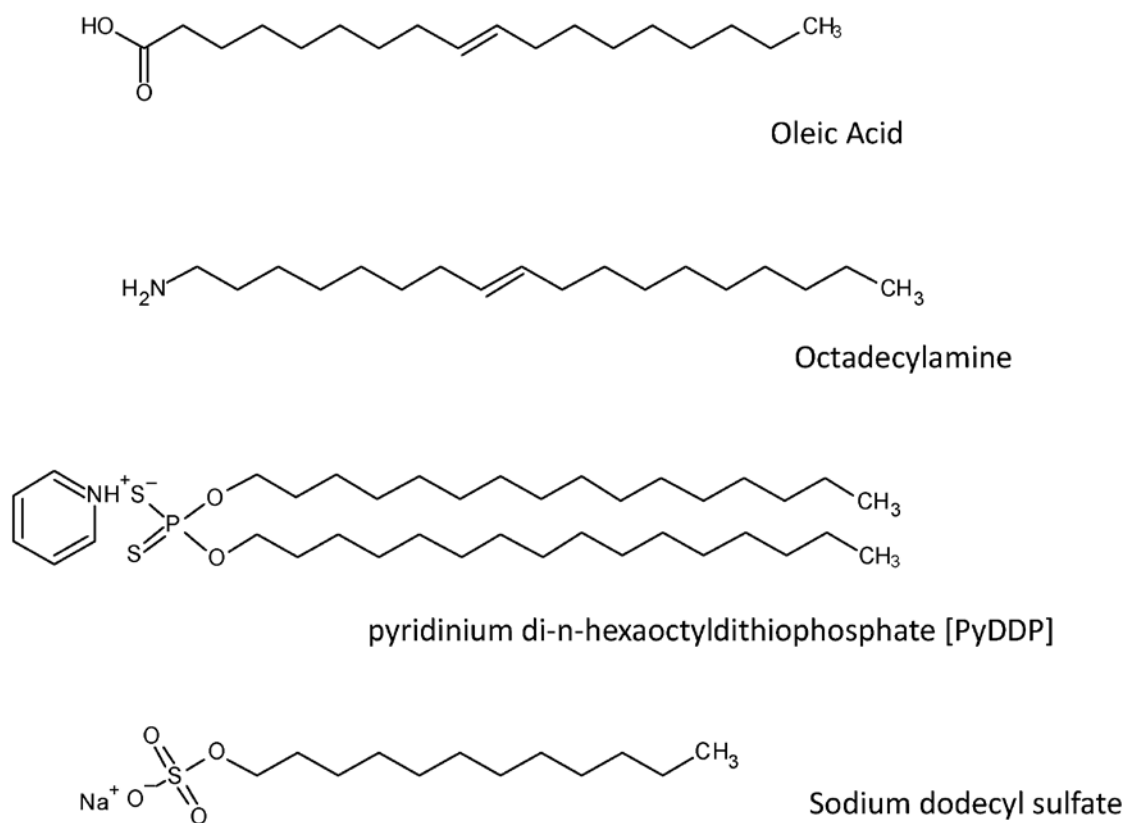


Figure 2. The chemical structure of some surfactants used in surfactant surface modifications.

To solve this problem, another modification method was developed. Instead of modifying nanoparticles, this method uses a surfactant to modify the precursor of nanoparticles first, which allows synthesizing of nanoparticles with a pre-attached surfactant. The tungsten sulfide nanoparticles synthesized using this method achieved remarkable dispersion stability in both room temperature and low temperature conditions [24]. This method can also synthesize other types of metal sulfide. However, their dispersion stability in lubricant and their tribological impact is still unknown [119].

The dispersion stability of surfactant-modified nanoparticles was also closely linked to their size. Nanoparticles under 10 nm in size show better stability of dispersion by using the surfactant surface modification method [10,24,53,55,57,74]. This result can be explained by the steric stabilization theory discussed in the next chapter.

2.2.2. Silanization

The surface silanization method is almost exclusively applicable to metal oxides and metal nanoparticles with surface oxidations. This method uses alkoxy silanes to modify the nanoparticle surface. Figure 3 presents a few examples of alkoxy silanes used to modify nanoparticles [10,16,19,21,40,41,110,113]. Similar to surfactants, alkoxy silane molecules have a functional group capable of reacting with nanoparticle surfaces (Si-CH₃), and a functional group that can stabilize the nanoparticles in oil. The surface silanization process can graft not just alkyl functional groups but also other functional groups like the amino group or the epoxide group.

Typical treatment of TiO₂ or SiO₂ nanoparticles was mixing the alkoxy silanes and nanoparticles in a basic solvent at an elevated temperature [10,16,19,21,40,41,110]. Two chemical processes would

occur during the surface silanization process: formation of Si-O-Metal bonds on a nanoparticle's surface through hydrolysis and condensation of silane alkoxy groups, and oligomerization between two alkoxy silane molecules [120–122]. These two competing chemical processes created a structure on the surface layer which had a complex conformation (Figure 4). Studies surveyed in Table 1 all used silanes with three silanes functional group and long reaction times under aqueous solvent. Under this condition, a thick interlinking layer formed [121]. However, even with this thick layer, the nanoparticles functionalized with the amino group still had poor stability compared to the nanoparticles functionalized with alkyl chains in lubricant oil [41].

For nanoparticles which have little or no surface hydroxyl group, it was difficult to directly use silanes to perform surface modification. The IF-WS₂ treated with ODTS (octadecyltrichlorosilane) could only be stabilized in liquid paraffin for less than one week [23], but similar sized silica nanoparticles with similar treatment could be stable for more than 4 months [41]. Surface oxidation [110,118] or coating the surface of nanoparticle with silica [123] are alternative methods.

Even though nanoparticles with long alkyl chains grafted on its surface could form more stable dispersion in lubricant oil, the alkoxy silanes with long alkyl chains were not used by majority of the research reviewed. This was likely because those types of alkoxy silanes were more expensive compared to amino silanes, such as APTEOS ((3-Aminopropyl)triethoxysilane) or DETAS (N1-(3-Trimethoxysilylpropyl)diethylenetriamine).

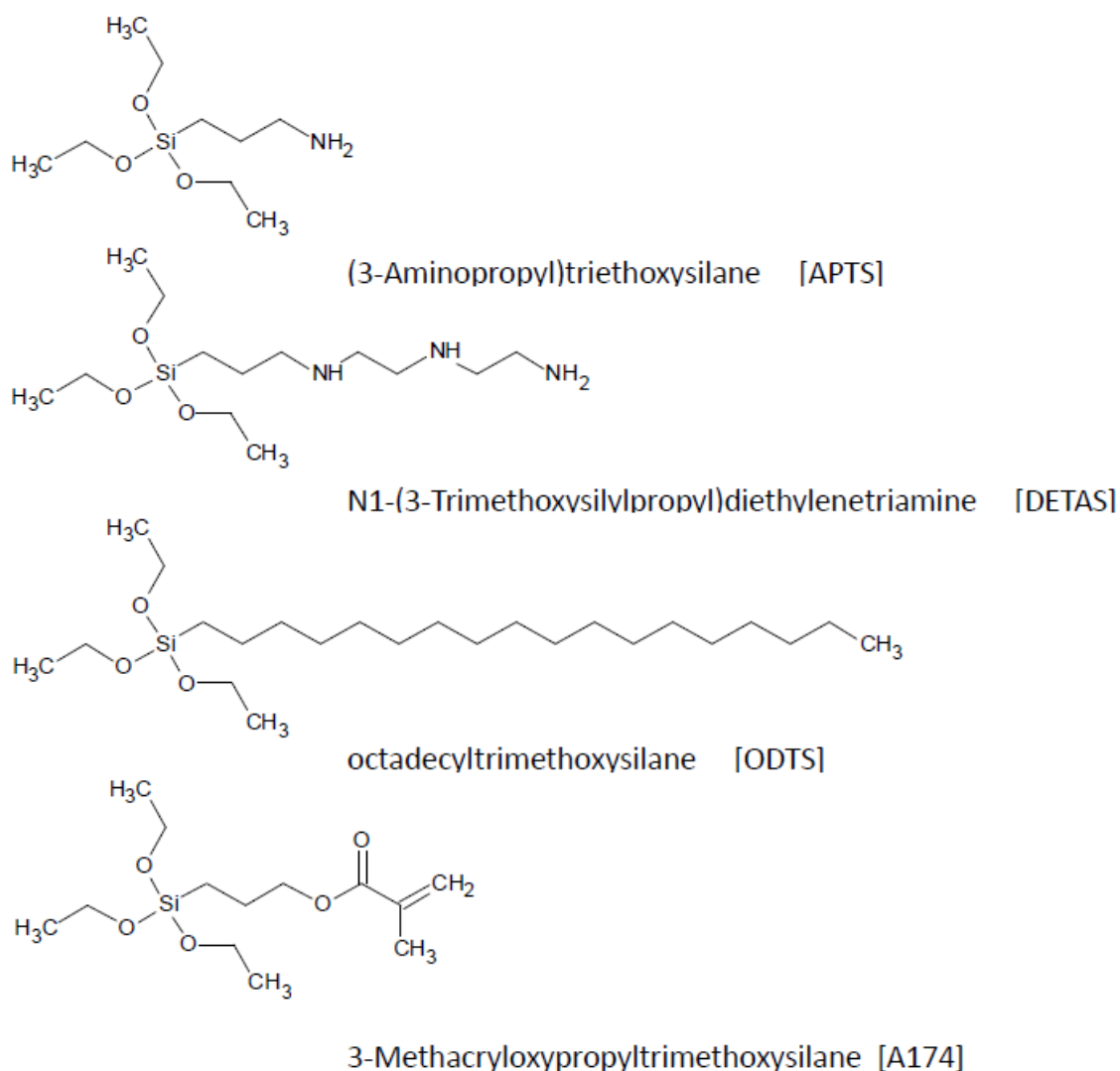


Figure 3. The structure of silanes used to modify the surface of nanoparticles.

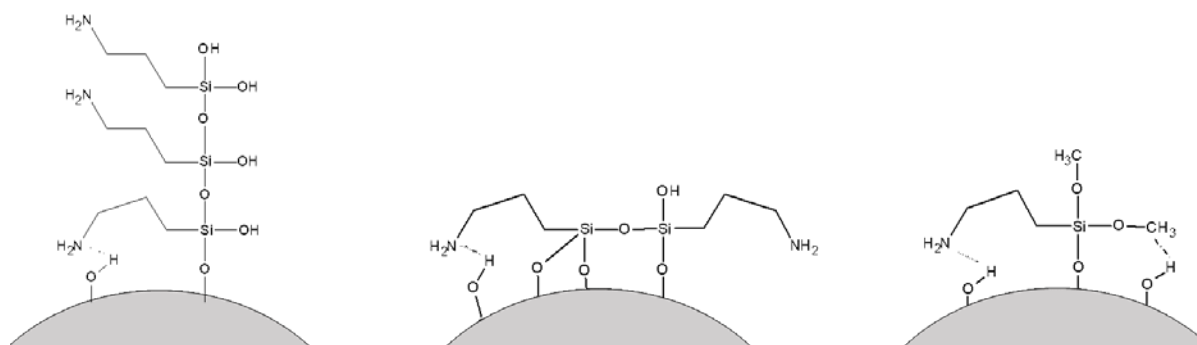


Figure 4. The Structure of APS ((3-Aminopropyl)triethoxysilane) treated silica nanoparticle surface (Redraw based on Reference [106]).

A two-step functionalization method was developed to solve this problem. The first step of the modification was the grafting of alkoxy silanes with an amino group. APTEOS [17,124] or DETAS [16,40] was used in this process. The second step was to bond a carboxylic acid surfactant, such as lauric acid [17] or stearic acid [16,40,124], to the amino group. This method grafted long alkyl chains on the silica surface without the use of expensive ODTS (octadecyltrichlorosilane). This method can result in a thicker grafted layer with a preferred chemical structure.

In contrast to the surfactant surface modification, all the nanoparticles which used surface silanization were larger than 10 nm in size. The large curvature of small nanoparticles could limit the reaction between alkoxy silane and a hydroxyl group, reducing the grafting density [125]. Additionally, almost all the papers reviewed used an excessive amount of silane in the surface modification process. However, this practice could cause irreversible aggregation of nanoparticles in the modification process when small nanoparticles were used [126].

2.3. Other Methods

Some recent work reported the adaption of the silane modification method to develop nanolubricants based on surface-induced-atom-transfer-radical polymerization (SI-ATRP) and nanoscale ionic material (NIM).

The SI-ATRP method can graft a long chain polymer on the surface of nanoparticles [11,14,127,128]. Instead of grafting long chain molecules on the nanoparticle surface, this method grafted silanes with initiator groups. This initiator was then used to react with monomers, forming a polymer chain on the surface [11,14]. This method could graft polymers with more than 100 C–C bonds [11], an order of magnitude higher compared to the results from the surfactant modification or surface silanization methods. It also achieved remarkable dispersion stability. The TiO_2 and SiO_2 particle treated with this method could stay stable over a large temperature range ($-20\text{ }^\circ\text{C}$ to $140\text{ }^\circ\text{C}$) for a long period of time (>2 months) [11,14].

The NIM method employed a two-step surface modification process. For the first step of the surface modification, an ionic corona was tethered on nanoparticles by surface silanization or ion exchange. For the second step, an organic counter-ion was linked to the surface [13,129]. This formed a liquid-like material which could disperse into both polar and non-polar solvents [83].

Essentially, those two methods further altered the nanoparticles' physical and chemical properties forming a new type of nanomaterials.

2.4. Evaluation

The methods discussed have different effectiveness and reliability. In Figure 5 the reported minimum stabilizing time is plotted. In the figure, each marker represents one report on the stable time of one type of nanoparticle. According to the aggregated data, modifying the nanoparticle surface is undeniably more effective compared to dispersing nanoparticles directly or formulating the oil

with dispersant. Among the surface modification methods, the surface silanization method appears more reliable.

In comparison to the types of materials, oxides appear to have the longest stable time. Due to the abundance of the hydroxyl group on their surface, oxide is well suited to be modified by both surfactant and silane [115,125,130]. In existing reports, there was only one non-oxide nanoparticle additive suspended for more than 1 month [24]. This was made possible by adding surfactant to modify the precursors of WS₂ nanoparticles with oleyamin. This may suggest that the difficulty in forming a stable dispersion with non-oxide particles can be solved with suitable surface modification methods.

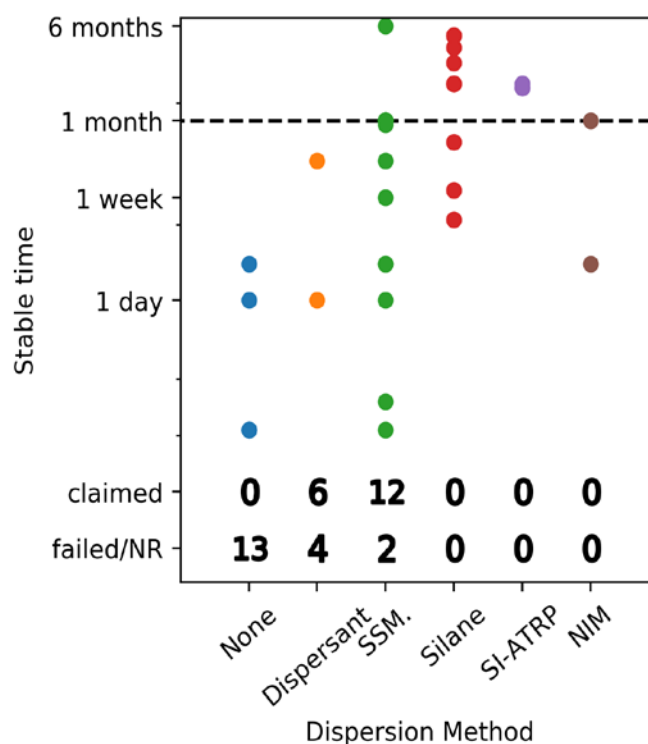


Figure 5. The stable time for different method from surveyed studies in Table 1. Every marker represents one least stable time reported by the papers. The “claimed” in this figure referred to the researches provide no stable time but claimed to be stable. The “failed/NR” in this figure refers to the researches failed to form a stable dispersion or did not report dispersion stability.

3. Theory

3.1. Some Basics

The dispersion of nanoparticles can be explained by colloidal theories [131]. The dispersed particles studied in colloidal science ranged between 1 nm and 1000 nm in size, a range which overlaps the size of nanoparticles.

In colloidal theories, the tendency in aggregation of nanoparticles was determined by two factors: the thermal agitation particles received from the solvent and the interaction between nanoparticles. The thermal agitation in the solvent has an energy of $K_b T$, where K_b is Boltzmann constant and T is temperature. This thermal agitation was shown to push the nanoparticles to move randomly in the solvent, causing the famous Brownian motion [132]. The interaction between particles resulted in the attractive and repulsive forces between two particles [132]. Stable dispersion formed when the thermal agitation overcame the attractive force between particles.

The DLVO (Derjaguin and Landau 1941, Verwey and Overbeek 1948) theory has been widely accepted to explain the colloidal stability of particles. It explained the dispersion stabilization through attractive van der Waals forces and repulsive screened electrostatic forces [132]. The van der Waals

force originate from the polarization of particles. These polarized particles act as electric dipoles which attract each other and aggregate if no repulsive force exists. This tendency of aggregation is opposed by the electrostatic force between the particles. Although this force is weak in a non-polar solvent, it is enhanced through ion screening process in polar solvent [133,134]. However, the polarity of lubricants renders electrostatic stabilization difficult in lubricant oil. In the context of colloidal dispersion, the dielectric constant (ϵ) can be used to measure polarity. In organic media, with $\epsilon \leq 5$ the electrostatic interaction is weak even when nanoparticles have surface charge [133,135]. Most lubricants' dielectric constant are around 2.5 [136], far lower than the dielectric constants of water or other polar solvents. Thus, the surface charge of nanoparticles cannot improve dispersion in the lubricant oil. In some of the surveyed publications, ζ -potential (surface potential) is characterized and used to reflect the dispersion stability [40–42]. However, it is incorrect for proving dispersion stability using this characterization because surface potential contributes little to the particles' interactions in lubricant oil.

Another widely adapted theory is "steric stabilization" [137–139]. This theory states that a grafted particle generates a repulsive force when another particle approaches it. With sufficient repulsive force acting against the van der Waals potential, a balanced state is possible resulting stable suspension. In the following, further discussion about this theory is carried out.

3.2. Steric Stabilization

Steric stabilization is established by the balance between two forces: the van der Waals attractive force and the elastic steric force [137–140]. Although van der Waals force is complex in nature, a simplified form by Hamaker was used when analyzing colloidal systems [141]. Assuming the size of the nanoparticles are small compared with the average distance between them, we use London van der Waals potential [141]:

$$V_{vdw}(z, R) = -\frac{A}{6} \left(\frac{2R^2}{z^2 - R^2} + \frac{2R^2}{z^2} + \ln \left(\frac{z^2 - 4R^2}{z^2} \right) \right) \quad (1)$$

Here z is the distance between two particles' centers, R is the radius of the particle and A is the effective Hamaker constant. The effective Hamaker constant can be approximated by the Hamaker constant of the particles and the medium [132]:

$$A = \left(\sqrt{A_{particle}} - \sqrt{A_{medium}} \right)^2 \quad (2)$$

The nanoparticles have a Hamaker constant of $10^{-20} - 10^{-19}$ J [142] and the organic media has a Hamaker constant normally about 10^{-20} J [143–145]. For example, the Hamaker constant of Silica in vacuum is 6.35×10^{-20} J [142]. Compared to inorganic compound, the metals have a larger Hamaker constant 22×10^{-20} J [146]. Their Hamaker constants also increases with decrease in size [147,148]. The Hamaker constant of a 5 nm sized Ag nanoparticle is 34×10^{-20} J [148], larger than that of bulk material. Thus, an effective Hamaker constant of $10^{-20} - 10^{-19}$ J is used to analyze the van der Waals attraction in lubricant oil.

The repulsive force originates from the deformation of the absorbed or grafted surface layer. When two particles with surface grafted layers approach, the surface layer deforms, and the conformation of the grafted molecule changes (Figure 6). This leads to the change of the free energy and the repulsive force [139]: $f = \frac{d\Delta F}{dH}$, here, f is the repulsive force, ΔF is the free energy of the surface layer, and H is the height of this polymer layer. In small deformations, the elastic potential between two approaching particles are (modified from Reference [139] Equation (54)):

$$\Delta V_{steric} \cong \frac{d}{2} \left(\frac{H_0 - H/2}{r} \right) \Delta F(H/2) \quad \text{when } H < 2H_0 \quad (3)$$

Here, d is the density of grafted chains, H_0 is the thickness of the grafted layer, r is particle radius, ΔF is the free energy of one molecule, and H is the distance between particles. A potential well appears when van der Waals potential and steric potential are combined (Figure 6a). If the thermal agitation is larger than this potential well, a stable dispersion can be expected.

A qualitative analysis on Equation (3) leads to the major factor influencing steric stability: the size of the particles, the thickness of the surface layer, the density of grafted chains, and the free energy of the grafted chains. These factors are discussed in following sections.

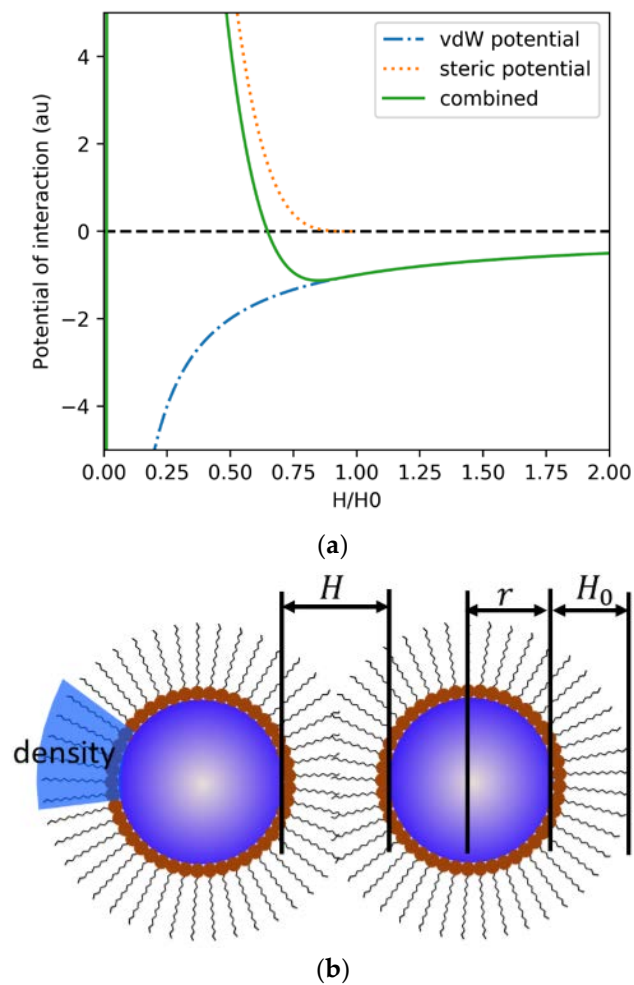


Figure 6. The model of steric repulsion, (a) The van der Waals potential, elastic steric potential, and the combination of the two. Value plotted based on Equations (1) and (3). (b) The figure diagrammatically represents the afore mentioned.

3.3. Size Effects

The theoretical analysis from the previous chapter indicates that when the same surface modification is used, a reduction in the size of nanoparticles will decrease the attractive van der Waals force and increase the repulsive steric force. The result from the surfactant surface modification best illustrates this size effect. In Figure 7, the stable time of seven different research articles using a similar surfactant surface modification method is plotted against the size of the nanoparticle used in their research. It appears that the nanoparticles with a size smaller than 10 nm have better stability compared to the nanoparticles with a size larger than 10 nm.

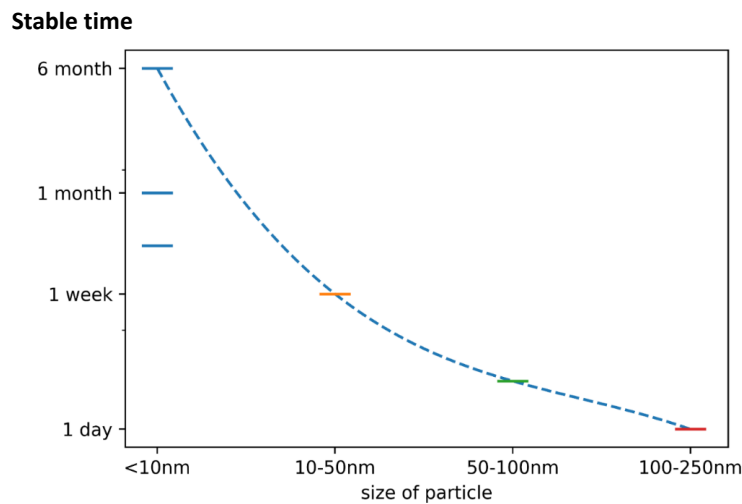


Figure 7. The nanoparticle size and nanoparticle dispersion stability in 10 researches (from up to bottom, left to right: [24], [10,43], [55], [74], [57], [53]) using surfactant surface modification.

A simple estimation based on colloidal theory can explain this phenomenon. The potential well of the steric stabilization is correlated to the size of interacting particles. There is no elastic steric force beyond the thickness of the surface polymer layer. Thus, one minimum of the potential energy is around the thickness of the surface layer. The value of this minimum is smaller than the value of van der Waals potential. Only considering these two factors (surface layer thickness and van der Waals potential), an upper limit of the nanoparticle that can be stabilized by a surface layer of thickness H_0 . The estimated upper limit of a nanoparticle is the root of R in:

$$V_{vdw}(H_0, R) - k_bT = 0 \tag{4}$$

The surface layer thickness H_0 of surface modification by surfactant is about 3 nm [149,150]. The estimated upper limit is plotted in Figure 8. This estimation is in agreement with the literature surveyed in this paper (Table 1).

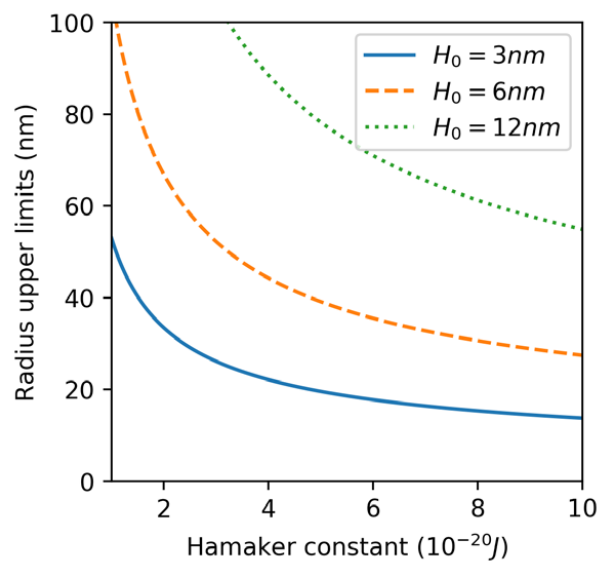


Figure 8. The upper limit of nanoparticles that can be stabilized with a grafted layer thickness of H_0 . The blue line can be used for surfactant surface modification because the thickness of organic layer grafted by surfactant surface modification was about 3 nm [149,150].

However, according to Figure 7, the nanoparticles with a radius less than 200 nm still have poor stability. Both the van der Waals and the steric forces need to be considered to explain this [139]. In Figure 9, the potential of particle–particle interaction is plotted against the distance between two particles. All three figures are based on the nanoparticles with the same parameters except the particle radius. The steric potential was calculated using models proposed in Reference [109]. In this figure, the potential is normalized by the free energy of the surface molecule layer, and distance is normalized by the thickness of the grafted layer under θ conditions. The diameter of the nanoparticle was the only different parameter in those three calculations. With the increase of nanoparticle size, the total repulsive force decreased until it totally vanished.

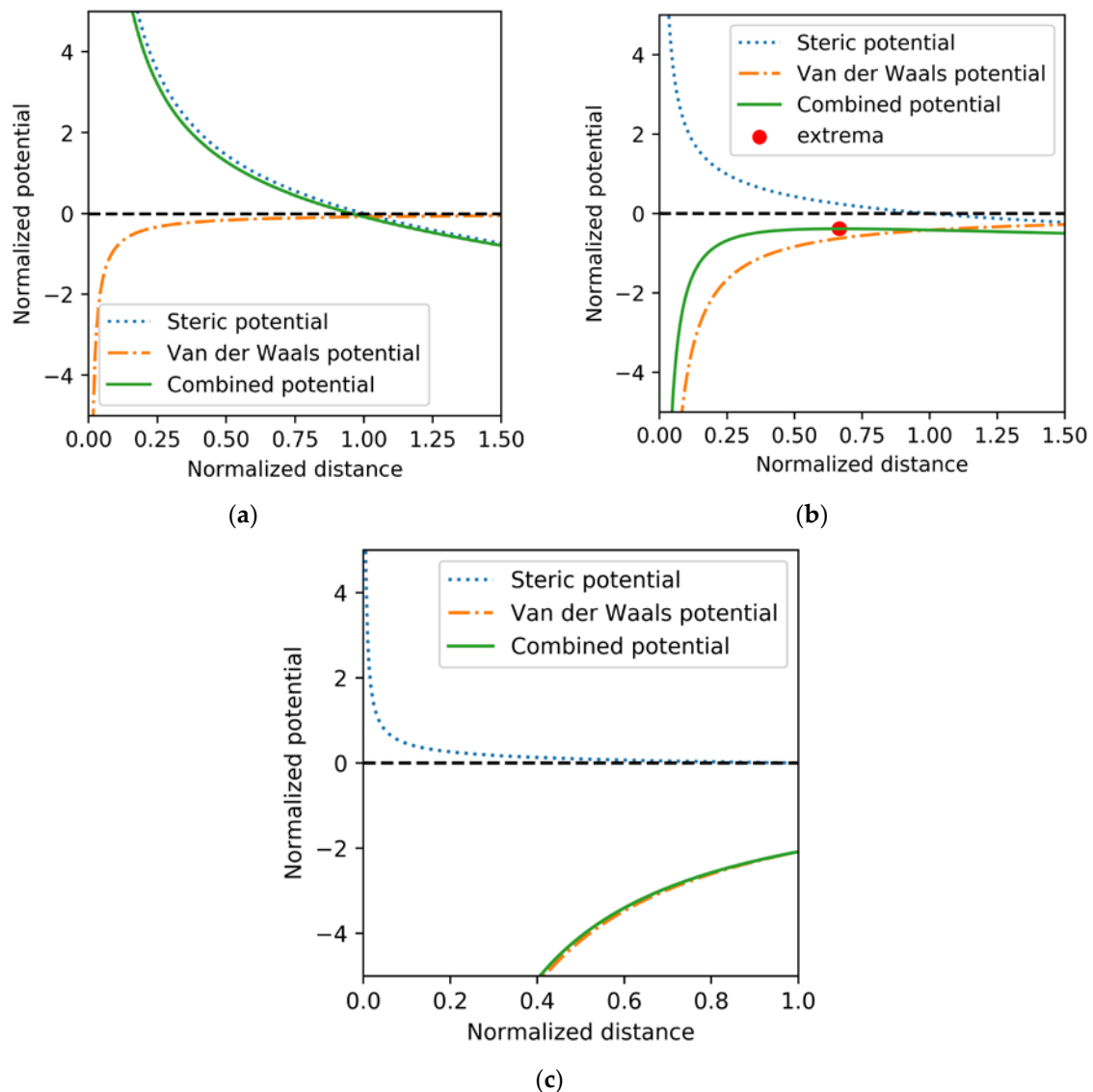


Figure 9. The van der Waals, steric, and combined potential between two nanoparticles with (a) radius of 2 times the grafted layer thickness; (b) radius of 10 times the grafted layer thickness; (c) radius of 30 times the grafted layer thickness.

3.4. Grafted Surface Layers

The properties of the grafted layer are believed to influence the ability of nanoparticles to disperse in organic media [40,41,116,149]. For the same nanoparticle, a change in the grafting density, the thickness of the surface grafted layer or the free energy can alter the strength of the repulsive force in Equation (4).

The effectiveness of the surface modification method requires a sufficient grafting density. In the case of surfactant surface modification, an increase in the concentration of surfactant used has a positive impact on the dispersion stability [115,116,149]. When the nanoparticle reacted with the surfactant in the solvent, if the nanoparticle aggregated and does not fully react with the surfactant, its re-dispersibility is impeded [114]. This is the reason why surface silanization is suitable for nanoparticles larger than 50 nm size. The high curvature of nanoparticles smaller than 30 nm leads to poor grafting density of silane [125]. This poor grafting density causes the low steric repulsion force, and the dispersion stability is reduced.

The chemical composition of the interface between nanoparticles and grafted layers can influence the grafting density and the stability of nanolubricants. Nanoparticles modified with silane provide overall better dispersion [16,19,21,40,41] compared with nanoparticles modified with surfactant [10,53,57,67,74,106]. Both silane and surfactant can react with the hydroxyl group to form a bond with the nanoparticle surface [115,116,149,151,152]. However, compared with surfactant, silane can fully react with the hydroxyl group on the surface of nanoparticles. In the case of silica nanoparticle treatment, the research using an oleic acid surface modification of the hydroxyl group did not fully react even with the excess amount of reactant [115]. In contrast, the silica nanoparticles modified with silane coupling agent have almost no hydroxyl group left after the reaction [151]. Moreover, the conformation of the grafted layer changes when the surface density increases [153]. The grafted layer had a “mushroom-like” conformation when the grafting is low but changes to “brush-like” with a high grafting density [153]. This results in a higher $\Delta F(H)$ value in Equation (4), increasing the steric repulsive force.

Another factor affecting suspension is the chemical composition of the grafted molecule chain. Steric stabilization is far more effective when the dispersant is a good solvent of the molecules grafted on the nanoparticle [138,139]. A good solvent can also expand the grafted layer beyond the θ -condition, resulting in a thicker layer with a higher interaction force [139]. The nanoparticles grafted with the alkyl group show better stability compared to nanoparticles grafted with the amino, phenyl or carboxyl groups [16,40]. This is due to the high-solubility of the alkyl group in the hydrocarbon lubricant [116]. Even changing the property of the end group of the grafted layer can alter the nanoparticles' dispersion ability. Fe_3O_4 modified with oleic acid can disperse well in a non-polar solvent, but not in a polar solvent. Changing the end group of oleic acid to oleate reverses the dispersion behavior, resulting in a good dispersion in polar solvent instead of non-polar solvent [149].

According to Equation (3) and previous analysis of particle sizes, the thick surface layer is beneficial to the stability of nanoparticles (Figure 8). The study on TiO_2 with amine surfactant found that increasing the number of carbon atoms in grafted surfactant from 3 to 12 increases the dispersibility in a non-polar solvent [114]. However, both the surfactant surface modification method and the surface modification method result in a surface layer with similar thickness [122,149]. The only method which has significantly thicker surface layer is the SI-ATRP method. This method can graft the longest chain on the surface of nanoparticles [11,14]. This explains the high stability of nanoparticles modified by this method. Even in temperatures lower than -20 Celsius, the nanoparticle dispersion can stay stable for more than 2 months [11,14].

4. Conclusions

In this review, the approach and theory of nanoparticle dispersion in lubricant oils were critically analyzed. Dispersion of nanoparticles was studied using colloidal theory. The influence of material, particle size, and surface modification on dispersion were examined. The findings are summarized below.

Surface modification is essential to disperse nanoparticles into a lubricating oil. Theoretical analysis indicated that steric stabilization played important roles in oils, more so than other mechanisms due to the non-polar nature. Steric stabilization is promoted by formulating oil with a dispersant

or particle modification to form an organic surface layer. However, the use of dispersant is limited because it hinders the friction modification of nanoparticles.

To obtain a stable suspension, it is essential for the surface of nanoparticles to have long alkyl chains with sufficient grafting density and thickness-to-size ratio. For particles with sizes under 50 nm, using surfactants to modify their surfaces results in desirable suspension. For oxide particles larger than 10 nm, surface silanization has a clear advantage because of its higher grafting density and versatility.

Acknowledgments: This research was partially supported by the TTRF (Taiho Kogyo Tribology Research Foundation). P.R. was sponsored by the NSF graduate fellowship (award number 2018265813).

Conflicts of Interest: The authors declare no conflicts of interest.

References

1. Holmberg, K.; Erdemir, A. Influence of tribology on global energy consumption, costs and emissions. *Friction* **2017**, *5*, 263–284. [[CrossRef](#)]
2. Holmberg, K.; Andersson, P.; Erdemir, A. Global energy consumption due to friction in passenger cars. *Tribol. Int.* **2012**, *47*, 221–234. [[CrossRef](#)]
3. Holmberg, K.; Andersson, P.; Nylund, N.-O.; Mäkelä, K.; Erdemir, A. Global energy consumption due to friction in trucks and buses. *Tribol. Int.* **2014**, *78*, 94–114. [[CrossRef](#)]
4. Holmberg, K.; Kivikytö-Reponen, P.; Härkisaari, P.; Valtonen, K.; Erdemir, A. Global energy consumption due to friction and wear in the mining industry. *Tribol. Int.* **2017**, *115*, 116–139. [[CrossRef](#)]
5. Dai, W.; Kheireddin, B.; Gao, H.; Liang, H. Roles of nanoparticles in oil lubrication. *Tribol. Int.* **2016**, *102*, 88–98. [[CrossRef](#)]
6. Gulzar, M.; Masjuki, H.H.; Kalam, M.A.; Varman, M.; Zulkifli, N.W.M.; Mufti, R.A. Tribological performance of nanoparticles as lubricating oil additives. *J. Nanoparticle Res.* **2016**, *18*, 223. [[CrossRef](#)]
7. Chinas-Castillo, F.; Spikes, H.A. Mechanism of action of colloidal solid dispersions. *J. Tribol.* **2003**, *125*, 552–557. [[CrossRef](#)]
8. Kalin, M.; Kogovšek, J.; Remškar, M. Mechanisms and improvements in the friction and wear behavior using MoS₂ nanotubes as potential oil additives. *Wear* **2012**, *280–281*, 36–45. [[CrossRef](#)]
9. Rabaso, P.; Ville, F.; Dassenoy, F.; Diaby, M.; Afanasiev, P.; Cavoret, J.; Vacher, B.; Le Mogne, T. Boundary lubrication: Influence of the size and structure of inorganic fullerene-like MoS₂ nanoparticles on friction and wear reduction. *Wear* **2014**, *320*, 161–178. [[CrossRef](#)]
10. Li, B.; Wang, X.; Liu, W.; Xue, Q. Tribochemistry and antiwear mechanism of organic–inorganic nanoparticles as lubricant additives. *Tribol. Lett.* **2006**, *22*, 79–84. [[CrossRef](#)]
11. Wright, R.A.E.; Wang, K.; Qu, J.; Zhao, B. Oil-Soluble Polymer Brush Grafted Nanoparticles as Effective Lubricant Additives for Friction and Wear Reduction. *Angew. Chem. Int. Ed.* **2016**, *55*, 8656–8660. [[CrossRef](#)] [[PubMed](#)]
12. Bogunovic, L.; Zuenkeler, S.; Toensing, K.; Anselmetti, D. An Oil-Based Lubrication System Based on Nanoparticulate TiO₂ with Superior Friction and Wear Properties. *Tribol. Lett.* **2015**, *59*, 29. [[CrossRef](#)]
13. Kim, D.; Archer, L.A. Nanoscale Organic–Inorganic Hybrid Lubricants. *Langmuir* **2011**, *27*, 3083–3094. [[CrossRef](#)] [[PubMed](#)]
14. Seymour, B.T.; Wright, R.A.; Parrott, A.C.; Gao, H.; Martini, A.; Qu, J.; Dei, S.; Zhao, B. Poly (alkyl methacrylate) Brush-Grafted Silica Nanoparticles as Oil Lubricant Additives: Effects of Alkyl Pendant Groups on Oil Dispersibility, Stability, and Lubrication Property. *ACS Appl. Mater. Interfaces* **2017**, *9*, 25038–25048. [[CrossRef](#)] [[PubMed](#)]
15. Xie, H.; Jiang, B.; He, J.; Xia, X.; Pan, F. Lubrication performance of MoS₂ and SiO₂ nanoparticles as lubricant additives in magnesium alloy-steel contacts. *Tribol. Int.* **2016**, *93*, 63–70. [[CrossRef](#)]
16. Sui, T.; Song, B.; Zhang, F.; Yang, Q. Effect of Particle Size and Ligand on the Tribological Properties of Amino Functionalized Hairy Silica Nanoparticles as an Additive to Polyalphaolefin. *J. Nanomater.* **2015**, *16*, 427. [[CrossRef](#)]
17. López, T.D.-F.; González, A.F.; Reguero, Á.D.; Matos, M.; Díaz-García, M.E.; Badía-Laíño, R. Engineered silica nanoparticles as additives in lubricant oils. *Sci. Technol. Adv. Mater.* **2015**, *16*, 055005. [[CrossRef](#)]

18. Sui, T.; Song, B.; Zhang, F.; Yang, Q. Effects of functional groups on the tribological properties of hairy silica nanoparticles as an additive to polyalphaolefin. *RSC Adv.* **2016**, *6*, 393–402. [[CrossRef](#)]
19. Jiao, D.; Zheng, S.; Wang, Y.; Guan, R.; Cao, B. The tribology properties of alumina/silica composite nanoparticles as lubricant additives. *Appl. Surf. Sci.* **2011**, *257*, 5720–5725. [[CrossRef](#)]
20. Chen, Q.; Zheng, S.; Yang, S.; Li, W.; Song, X.; Cao, B. Enhanced tribology properties of ZnO/Al₂O₃ composite nanoparticles as liquid lubricating additives. *J. Sol-Gel Sci. Technol.* **2012**, *61*, 501–508. [[CrossRef](#)]
21. Luo, T.; Wei, X.; Huang, X.; Huang, L.; Yang, F. Tribological properties of Al₂O₃ nanoparticles as lubricating oil additives. *Ceram. Int.* **2014**, *40*, 7143–7149. [[CrossRef](#)]
22. Zhou, Q.; Huang, J.; Wang, J.; Yang, Z.; Liu, S.; Wang, Z.; Yang, S. Preparation of a reduced graphene oxide/zirconia nanocomposite and its application as a novel lubricant oil additive. *RSC Adv.* **2015**, *5*, 91802–91812. [[CrossRef](#)]
23. Shahar, C.; Zbaida, D.; Rapoport, L.; Cohen, H.; Bendikov, T.; Tannous, J. Surface Functionalization of WS₂ Fullerene-like Nanoparticles. *Langmuir* **2010**, *26*, 4409–4414. [[CrossRef](#)]
24. Jiang, Z.; Zhang, Y.; Yang, G.; Yang, K.; Zhang, S.; Yu, L. Tribological Properties of Oleylamine-Modified Ultrathin WS₂ Nanosheets as the Additive in Polyalpha Olefin Over a Wide Temperature Range. *Tribol. Lett.* **2016**, *61*, 24. [[CrossRef](#)]
25. Wu, J.; Fu, X. A low-temperature solvothermal method to prepare hollow spherical WS₂ nanoparticles modified by TOA. *Mater. Lett.* **2007**, *61*, 4332–4335. [[CrossRef](#)]
26. Xu, Z.Y.; Xu, Y.; Hu, K.H.; Xu, Y.F.; Hu, X.G. Formation and tribological properties of hollow sphere-like nano-MoS₂ precipitated in TiO₂ particles. *Tribol. Int.* **2015**, *81*, 139–148. [[CrossRef](#)]
27. Zin, V.; Agresti, F.; Barison, S.; Colla, L.; Mercadelli, E.; Fabrizio, M.; Pagura, M. Tribological Properties of Engine Oil with Carbon Nano-horns as Nano-additives. *Tribol. Lett.* **2014**, *55*, 45–53. [[CrossRef](#)]
28. Berne, B.J.; Pecora, R. *Dynamic Light Scattering: With Applications to Chemistry, Biology, and Physics*; Courier Corporation: Chelmsford, MA, USA, 2000.
29. Lin, J.; Wang, L.; Chen, G. Modification of Graphene Platelets and their Tribological Properties as a Lubricant Additive. *Tribol. Lett.* **2011**, *41*, 209–215. [[CrossRef](#)]
30. Einstein, A. *Investigations on the Theory of the Brownian Movement*; Courier Corporation: Chelmsford, MA, USA, 1956.
31. van Roij, R. Defying gravity with entropy and electrostatics: Sedimentation of charged colloids. *J. Phys. Condens. Matter.* **2003**, *15*, S3569. [[CrossRef](#)]
32. Piazza, R. Settled and unsettled issues in particle settling. *Rep. Prog. Phys.* **2014**, *77*, 056602. [[CrossRef](#)]
33. Xue, Q.; Liu, W.; Zhang, Z. Friction and wear properties of a surface-modified TiO₂ nanoparticle as an additive in liquid paraffin. *Wear* **1997**, *213*, 29–32. [[CrossRef](#)]
34. Zhang, L.; Chen, L.; Wan, H.; Chen, J.; Zhou, H. Synthesis and Tribological Properties of Stearic Acid-Modified Anatase (TiO₂) Nanoparticles. *Tribol. Lett.* **2011**, *41*, 409–416. [[CrossRef](#)]
35. Ingole, S.; Charanpahari, A.; Kakade, A.; Umare, S.S.; Bhatt, D.V.; Menghani, J. Tribological behavior of nano TiO₂ as an additive in base oil. *Wear* **2013**, *301*, 776–785. [[CrossRef](#)]
36. Beel, A.; Gottschalk, M.; Huetten, A.; Toensing, K.; Anselmetti, D. Tribological Performance of TiO₂-Nanostructured Particles as Oil-Lubricant Additives for Different Iron-Carbon Alloys. *Mater. Today Proc.* **2017**, *4*, S75–S80. [[CrossRef](#)]
37. Kheireddin, B.A.; Lu, W.; Chen, I.-C.; Akbulut, M. Inorganic nanoparticle-based ionic liquid lubricants. *Wear* **2013**, *303*, 185–190. [[CrossRef](#)]
38. Seymour, B.T.; Fu, W.; Wright, R.A.E.; Luo, H.; Qu, J.; Dai, S.; Zhao, B. Improved Lubricating Performance by Combining Oil-Soluble Hairy Silica Nanoparticles and an Ionic Liquid as an Additive for a Synthetic Base Oil. *ACS Appl. Mater. Interfaces* **2018**, *10*, 15129–15139. [[CrossRef](#)] [[PubMed](#)]
39. Li, X.; Cao, Z.; Zhang, Z.; Dang, H. Surface-modification in situ of nano-SiO₂ and its structure and tribological properties. *Appl. Surf. Sci.* **2006**, *252*, 7856–7861. [[CrossRef](#)]
40. Sui, T.; Ding, M.; Ji, C.; Yan, S.; Wei, J.; Wang, A.; Zhao, F. Dispersibility and rheological behavior of functionalized silica nanoparticles as lubricant additives. *Ceram Int.* **2018**. [[CrossRef](#)]
41. Sui, T.; Song, B.; Wen, Y.; Zhang, F. Bifunctional hairy silica nanoparticles as high-performance additives for lubricant. *Sci. Rep.* **2016**, *6*, 22696. [[CrossRef](#)]
42. Li, W.; Zheng, S.; Cao, B.; Ma, S. Friction and wear properties of ZrO₂/SiO₂ composite nanoparticles. *J. Nanoparticle Res.* **2011**, *13*, 2129–2137. [[CrossRef](#)]

43. Alves, S.M.; Mello, V.S.; Faria, E.A.; Camargo, A.P.P. Nanolubricants developed from tiny CuO nanoparticles. *Tribol. Int.* **2016**, *100*, 263–271. [[CrossRef](#)]
44. Hernández Battez, A.; González, R.; Viesca, J.L.; Fernández, J.E.; Díaz Fernández, J.M.; Machado, A.; Chou, R.; Riba, J. CuO, ZrO₂ and ZnO nanoparticles as antiwear additive in oil lubricants. *Wear* **2008**, *265*, 422–428. [[CrossRef](#)]
45. Alves, S.M.; Barros, B.S.; Trajano, M.F.; Ribeiro, K.S.B.; Moura, E. Tribological behavior of vegetable oil-based lubricants with nanoparticles of oxides in boundary lubrication conditions. *Tribol. Int.* **2013**, *65*, 28–36. [[CrossRef](#)]
46. Zhou, G.; Zhu, Y.; Wang, X.; Xia, M.; Zhang, Y.; Ding, H. Sliding tribological properties of 0.45% carbon steel lubricated with Fe₃O₄ magnetic nano-particle additives in baseoil. *Wear* **2013**, *301*, 753–757. [[CrossRef](#)]
47. Hu, Z.S.; Dong, J.X.; Chen, G.X. Study on antiwear and reducing friction additive of nanometer ferric oxide. *Tribol. Int.* **1998**, *31*, 355–360. [[CrossRef](#)]
48. Luo, T.; Wei, X.; Zhao, H.; Cai, G.; Zheng, X. Tribology properties of Al₂O₃/TiO₂ nanocomposites as lubricant additives. *Ceram Int.* **2014**, *40*, 10103–10109. [[CrossRef](#)]
49. Chen, S.; Liu, W.; Yu, L. Preparation of DDP-coated PbS nanoparticles and investigation of the antiwear ability of the prepared nanoparticles as additive in liquid paraffin. *Wear* **1998**, *218*, 153–158. [[CrossRef](#)]
50. Rosentsveig, R.; Gorodnev, A.; Feuerstein, N.; Friedman, H.; Zak, A.; Fleischer, N.; Tannous, J.; Dassenoy, F.; Tenne, R. Fullerene-like MoS₂ Nanoparticles and Their Tribological Behavior. *Tribol. Lett.* **2009**, *36*, 175–182. [[CrossRef](#)]
51. Joly-Pottuz, L.; Dassenoy, F.; Belin, M.; Vacher, B.; Martin, J.M.; Fleischer, N. Ultralow-friction and wear properties of IF-WS₂ under boundary lubrication. *Tribol. Lett.* **2005**, *18*, 477–485. [[CrossRef](#)]
52. Moshkovith, A.; Perfiliev, V.; Verdyan, A.; Lapsker, I.; Popovitz-Biro, R.; Tenne, R. Sedimentation of IF-WS₂ aggregates and a reproducibility of the tribological data. *Tribol. Int.* **2007**, *40*, 117–124. [[CrossRef](#)]
53. Jifen, W.; Wensheng, Z.; Guifen, J. Preparation and tribological properties of tungsten disulfide hollow spheres assisted by methyltriethylammonium chloride. *Tribol. Int.* **2010**, *43*, 1650–1658. [[CrossRef](#)]
54. Cizaire, L.; Vacher, B.; Le Mogne, T.; Martin, J.M.; Rapoport, L.; Margolin, A.; Tenne, R. Mechanisms of ultra-low friction by hollow inorganic fullerene-like MoS₂ nanoparticles. *Surf. Coat. Technol.* **2002**, *160*, 282–287. [[CrossRef](#)]
55. Wu, X.; Gong, K.; Zhao, G.; Lou, W.; Wang, X.; Liu, W. MoS₂/WS₂ Quantum Dots as High-Performance Lubricant Additive in Polyalkylene Glycol for Steel/Steel Contact at Elevated Temperature. *Adv. Mater. Interfaces* **2018**, *5*, 1700859. [[CrossRef](#)]
56. Bakunin, V.N.; Kuzmina, G.N.; Kasrai, M.; Parenago, O.P.; Bancroft, G.M. Tribological behavior and tribofilm composition in lubricated systems containing surface-capped molybdenum sulfide nanoparticles. *Tribol. Lett.* **2006**, *22*, 289–296. [[CrossRef](#)]
57. Koshy, C.P.; Rajendrakumar, P.K.; Thottackkad, M.V. Evaluation of the tribological and thermo-physical properties of coconut oil added with MoS₂ nanoparticles at elevated temperatures. *Wear* **2015**, *330–331*, 288–308. [[CrossRef](#)]
58. Wu, X.; Gong, K.; Zhao, G.; Lou, W.; Wang, X.; Liu, W. Surface Modification of MoS₂ Nanosheets as Effective Lubricant Additives for Reducing Friction and Wear in Poly- α -olefin. *Ind. Eng. Chem. Res.* **2018**, *57*, 8105–8114. [[CrossRef](#)]
59. Fernández-Coppel, I.A.; Martín-Ramos, P.; Martín-Gil, J.; Pamies, R.; Avella, M.; Avilés, M.D. Synthesis and Exploration of the Lubricating Behavior of Nanoparticulated Mo₁₅S₁₉ in Linseed Oil. *Materials* **2018**, *11*, 1783. [[CrossRef](#)] [[PubMed](#)]
60. Kang, X.; Wang, B.; Zhu, L.; Zhu, H. Synthesis and tribological property study of oleic acid-modified copper sulfide nanoparticles. *Wear* **2008**, *265*, 150–154. [[CrossRef](#)]
61. Zhou, J.; Wu, Z.; Zhang, Z.; Liu, W.; Xue, Q. Tribological behavior and lubricating mechanism of Cu nanoparticles in oil. *Tribol. Lett.* **2000**, *8*, 213–218. [[CrossRef](#)]
62. Yang, G.; Chai, S.; Xiong, X.; Zhang, S.; Yu, L.; Zhang, P. Preparation and tribological properties of surface modified Cu nanoparticles. *Trans. Nonferrous Met. Soc. China* **2012**, *22*, 366–372. [[CrossRef](#)]
63. Choi, Y.; Lee, C.; Hwang, Y.; Park, M.; Lee, J.; Choi, C.; Jung, M. Tribological behavior of copper nanoparticles as additives in oil. *Curr. Appl. Phys.* **2009**, *9*, e124–e127. [[CrossRef](#)]
64. Liu, G.; Li, X.; Qin, B.; Xing, D.; Guo, Y.; Fan, R. Investigation of the Mending Effect and Mechanism of Copper Nano-Particles on a Tribologically Stressed Surface. *Tribol. Lett.* **2004**, *17*, 961–966. [[CrossRef](#)]

65. Viesca, J.L.; Hernández Battez, A.; González, R.; Chou, R.; Cabello, J.J. Antiwear properties of carbon-coated copper nanoparticles used as an additive to a polyalphaolefin. *Tribol. Int.* **2011**, *44*, 829–833. [[CrossRef](#)]
66. Li, Y.; Zhang, S.; Ding, Q.; Li, H.; Qin, B.; Hu, L. Understanding the synergistic lubrication effect of 2-mercaptobenzothiazolate based ionic liquids and Mo nanoparticles as hybrid additives. *Tribol. Int.* **2018**, *125*, 39–45. [[CrossRef](#)]
67. Chen, Y.; Zhang, Y.; Zhang, S.; Yu, L.; Zhang, P.; Zhang, Z. Preparation of Nickel-Based Nanolubricants via a Facile In Situ One-Step Route and Investigation of Their Tribological Properties. *Tribol. Lett.* **2013**, *51*, 73–83. [[CrossRef](#)]
68. Qiu, S.; Zhou, Z.; Dong, J.; Chen, G. Preparation of Ni nanoparticles and evaluation of their tribological performance as potential additives in oils. *J. Tribol.* **2001**, *123*, 441–443. [[CrossRef](#)]
69. Chou, R.; Battez, A.H.; Cabello, J.J.; Viesca, J.L.; Osorio, A.; Sagastume, A. Tribological behavior of polyalphaolefin with the addition of nickel nanoparticles. *Tribol. Int.* **2010**, *43*, 2327–2332. [[CrossRef](#)]
70. Kumara, C.; Luo, H.; Leonard, D.N.; Meyer, H.M.; Qu, J. Organic-Modified Silver Nanoparticles as Lubricant Additives. *ACS Appl. Mater. Interfaces* **2017**, *9*, 37227–37237. [[CrossRef](#)] [[PubMed](#)]
71. Ghaednia, H.; Hossain, M.S.; Jackson, R.L. Tribological Performance of Silver Nanoparticle-Enhanced Polyethylene Glycol Lubricants. *Tribol. Trans.* **2016**, *59*, 585–592. [[CrossRef](#)]
72. Li, D.; Hong, B.; Fang, W.; Guo, Y.; Lin, R. Preparation of Well-Dispersed Silver Nanoparticles for Oil-Based Nanofluids. *Ind. Eng. Chem. Res.* **2010**, *49*, 1697–1702. [[CrossRef](#)]
73. Sun, L.; Tao, X.; Zhao, Y.; Zhang, Z. Synthesis and Tribology Properties of Stearate-Coated Ag Nanoparticles. *Tribol. Trans.* **2010**, *53*, 174–178. [[CrossRef](#)]
74. Sun, L.; Zhang, Z.J.; Wu, Z.S.; Dang, H.X. Synthesis and characterization of DDP coated Ag nanoparticles. *Mater. Sci. Eng. A* **2004**, *379*, 378–383. [[CrossRef](#)]
75. Kolodziejczyk, L.; Martínez-Martínez, D.; Rojas, T.C.; Fernández, A.; Sánchez-López, J.C. Surface-modified Pd nanoparticles as a superior additive for lubrication. *J. Nanoparticle Res.* **2007**, *9*, 639–645. [[CrossRef](#)]
76. Sánchez-López, J.C.; Abad, M.D.; Kolodziejczyk, L.; Guerrero, E.; Fernández, A. Surface-modified Pd and Au nanoparticles for anti-wear applications. *Tribol. Int.* **2011**, *44*, 720–726. [[CrossRef](#)]
77. Kumara, C.; Leonard, D.N.; Meyer, H.M.; Luo, H.; Armstrong, B.L.; Qu, J. Palladium Nanoparticle-Enabled Ultrathick Tribofilm with Unique Composition. *ACS Appl. Mater. Interfaces* **2018**, *10*, 31804–31812. [[CrossRef](#)]
78. Zhao, Y.; Zhang, Z.; Dang, H. Fabrication and Tribological Properties of Pb Nanoparticles. *J. Nanoparticle Res.* **2004**, *6*, 47–51. [[CrossRef](#)]
79. Huang, H.D.; Tu, J.P.; Gan, L.P.; Li, C.Z. An investigation on tribological properties of graphite nanosheets as oil additive. *Wear* **2006**, *261*, 140–144. [[CrossRef](#)]
80. Sanes, J.; Avilés, M.-D.; Saurín, N.; Espinosa, T.; Carrión, F.-J.; Bermúdez, M.-D. Synergy between graphene and ionic liquid lubricant additives. *Tribol. Int.* **2017**, *116*, 371–382. [[CrossRef](#)]
81. Zhang, W.; Zhou, M.; Zhu, H.; Tian, Y.; Wang, K.; Wei, J. Tribological properties of oleic acid-modified graphene as lubricant oil additives. *J. Phys. Appl. Phys.* **2011**, *44*, 205303. [[CrossRef](#)]
82. Choudhary, S.; Mungse, H.P.; Khatri, O.P. Dispersion of alkylated graphene in organic solvents and its potential for lubrication applications. *J. Mater. Chem.* **2012**, *22*, 21032–21039. [[CrossRef](#)]
83. Yang, J.; Xia, Y.; Song, H.; Chen, B.; Zhang, Z. Synthesis of the liquid-like graphene with excellent tribological properties. *Tribol. Int.* **2017**, *105*, 118–124. [[CrossRef](#)]
84. Sarno, M.; Senatore, A.; Cirillo, C.; Petrone, V.; Ciambelli, P. Oil Lubricant Tribological Behaviour Improvement Through Dispersion of Few Layer Graphene Oxide. *J. Nanosci. Nanotechnol.* **2014**. [[CrossRef](#)]
85. Kumar, P.; Wani, M.F. Tribological Characterisation of Graphene Oxide as Lubricant Additive on Hypereutectic Al-25Si/Steel Tribopair. *Tribol. Trans.* **2018**, *61*, 335–346. [[CrossRef](#)]
86. Kinoshita, H.; Ono, H.; Alias, A.A.; Nishina, Y.; Fujii, M. Tribological properties of graphene oxide as a lubricating additive in water and lubricating oils. *Mech. Eng. J.* **2015**, *2*. [[CrossRef](#)]
87. Alazemi, A.A.; Etacheri, V.; Dysart, A.D.; Stacke, L.-E.; Pol, V.G.; Sadeghi, F. Ultrasoft Submicrometer Carbon Spheres as Lubricant Additives for Friction and Wear Reduction. *ACS Appl. Mater. Interfaces* **2015**, *7*, 5514–5521. [[CrossRef](#)] [[PubMed](#)]
88. Tao, X.; Jiazheng, Z.; Kang, X. The ball-bearing effect of diamond nanoparticles as an oil additive. *J. Phys. Appl. Phys.* **1996**, *29*, 2932. [[CrossRef](#)]
89. Marko, M.; Kyle, J.; Branson, B.; Terrell, E. Tribological Improvements of Dispersed Nanodiamond Additives in Lubricating Mineral Oil. *J. Tribol.* **2014**, *137*, 011802. [[CrossRef](#)]

90. Acharya, B.; Avva, K.S.; Thapa, B.; Pardue, T.N.; Krim, J. Synergistic Effect of Nanodiamond and Phosphate Ester Anti-Wear Additive Blends. *Lubricants* **2018**, *6*, 56. [[CrossRef](#)]
91. Chou, C.-C.; Lee, S.-H. Tribological behavior of nanodiamond-dispersed lubricants on carbon steels and aluminum alloy. *Wear* **2010**, *269*, 757–762. [[CrossRef](#)]
92. Lee, J.; Cho, S.; Hwang, Y.; Lee, C.; Kim, S.H. Enhancement of Lubrication Properties of Nano-oil by Controlling the Amount of Fullerene Nanoparticle Additives. *Tribol. Lett.* **2007**, *28*, 203–208. [[CrossRef](#)]
93. Joly-Pottuz, L.; Vacher, B.; Ohmae, N.; Martin, J.M.; Epicier, T. Anti-wear and Friction Reducing Mechanisms of Carbon Nano-onions as Lubricant Additives. *Tribol. Lett.* **2008**, *30*, 69–80. [[CrossRef](#)]
94. Joly-Pottuz, L.; Bucholz, E.W.; Matsumoto, N.; Phillpot, S.R.; Sinnott, S.B.; Ohmae, N. Friction Properties of Carbon Nano-Onions from Experiment and Computer Simulations. *Tribol. Lett.* **2009**, *37*, 75. [[CrossRef](#)]
95. Matsumoto, N.; Mistry, K.K.; Kim, J.-H.; Eryilmaz, O.L.; Erdemir, A.; Kinoshita, H. Friction reducing properties of onion-like carbon based lubricant under high contact pressure. *Tribol. Mater. Surf. Interfaces* **2012**, *6*, 116–120. [[CrossRef](#)]
96. Nunn, N.; Mahbooba, Z.; Ivanov, M.G.; Ivanov, D.M.; Brenner, D.W.; Shenderova, O. Tribological properties of polyalphaolefin oil modified with nanocarbon additives. *Diam. Relat. Mater.* **2015**, *54*, 97–102. [[CrossRef](#)]
97. Cornelio, J.A.C.; Cuervo, P.A.; Hoyos-Palacio, L.M.; Lara-Romero, J.; Toro, A. Tribological properties of carbon nanotubes as lubricant additive in oil and water for a wheel–rail system. *J. Mater. Res. Technol.* **2016**, *5*, 68–76. [[CrossRef](#)]
98. Khalil, W.; Mohamed, A.; Bayoumi, M.; Osman, T.A. Tribological properties of dispersed carbon nanotubes in lubricant. *Fuller Nanotub. Carbon Nanostruct.* **2016**, *24*, 479–485. [[CrossRef](#)]
99. Salah, N.; Abdel-wahab, M.S.; Habib, S.S.; Khan, Z.H. Lubricant Additives Based on Carbon Nanotubes Produced from Carbon-Rich Fly Ash. *Tribol. Trans.* **2017**, *60*, 166–175. [[CrossRef](#)]
100. Pamies, R.; Espejo, C.; Carrión, F.J.; Morina, A.; Neville, A.; Bermúdez, M.D. Rheological behavior of multiwalled carbon nanotube-imidazolium tosylate ionic liquid dispersions. *J. Rheol.* **2017**, *61*, 279–289. [[CrossRef](#)]
101. Wang, Z.; Ren, R.; Song, H.; Jia, X. Improved tribological properties of the synthesized copper/carbon nanotube nanocomposites for rapeseed oil-based additives. *Appl. Surf. Sci.* **2018**, *428*, 630–639. [[CrossRef](#)]
102. Qiu, S.; Dong, J.; Chen, G. Wear and friction behaviour of CaCO₃ nanoparticles used as additives in lubricating oils. *Lubr. Sci.* **2000**, *12*, 205–212. [[CrossRef](#)]
103. Zhang, M.; Wang, X.; Fu, X.; Xia, Y. Performance and anti-wear mechanism of CaCO₃ nanoparticles as a green additive in poly-alpha-olefin. *Tribol. Int.* **2009**, *42*, 1029–1039. [[CrossRef](#)]
104. Peri, J.B. The state of dispersion of detergent additives in lubricating oil and other hydrocarbons. *J. Am. Oil Chem. Soc.* **1958**, *35*, 110–117. [[CrossRef](#)]
105. Dong, J.X.; Hu, Z.S. A study of the anti-wear and friction-reducing properties of the lubricant additive, nanometer zinc borate. *Tribol. Int.* **1998**, *31*, 219–223. [[CrossRef](#)]
106. Song, X.; Zheng, S.; Zhang, J.; Li, W.; Chen, Q.; Cao, B. Synthesis of monodispersed ZnAl₂O₄ nanoparticles and their tribology properties as lubricant additives. *Mater. Res. Bull.* **2012**, *47*, 4305–4310. [[CrossRef](#)]
107. Zhang, Z.; Liu, W.; Xue, Q. Study on lubricating mechanisms of La(OH)₃ nanocluster modified by compound containing nitrogen in liquid paraffin. *Wear* **1998**, *218*, 139–144. [[CrossRef](#)]
108. Hu, Z.S.; Dong, J.X.; Chen, G.X.; He, J.Z. Preparation and tribological properties of nanoparticle lanthanum borate. *Wear* **2000**, *243*, 43–47. [[CrossRef](#)]
109. Zhou, J.; Wu, Z.; Zhang, Z.; Liu, W.; Dang, H. Study on an antiwear and extreme pressure additive of surface coated LaF₃ nanoparticles in liquid paraffin. *Wear* **2001**, *249*, 333–337. [[CrossRef](#)]
110. Kumari, S.; Sharma, O.P.; Gusain, R.; Mungse, H.P.; Kukrety, A.; Kumar, N.; Sugimura, H. Alkyl-Chain-Grafted Hexagonal Boron Nitride Nanoplatelets as Oil-Dispersible Additives for Friction and Wear Reduction. *ACS Appl. Mater. Interfaces* **2015**, *7*, 3708–3716. [[CrossRef](#)] [[PubMed](#)]
111. Farrokhpay, S. A review of polymeric dispersant stabilisation of titania pigment. *Adv. Colloid Interface Sci.* **2009**, *151*, 24–32. [[CrossRef](#)]
112. Rabaso, P.; Dassenoy, F.; Ville, F.; Diaby, M.; Vacher, B.; Mogne, T.L.; Belin, M. An Investigation on the Reduced Ability of IF-MoS₂ Nanoparticles to Reduce Friction and Wear in the Presence of Dispersants. *Tribol. Lett.* **2014**, *55*, 503–516. [[CrossRef](#)]
113. Kim, S.; Thiessen, P.A.; Bolton, E.E.; Chen, J.; Fu, G.; Gindulyte, A. PubChem Substance and Compound databases. *Nucleic Acids Res.* **2016**, *44*, D1202–D1213. [[CrossRef](#)]

114. Nakayama, N.; Hayashi, T. Preparation of TiO₂ nanoparticles surface-modified by both carboxylic acid and amine: Dispersibility and stabilization in organic solvents. *Colloids Surf. Physicochem. Eng. Asp.* **2008**, *317*, 543–550. [[CrossRef](#)]
115. Li, Z.; Zhu, Y. Surface-modification of SiO₂ nanoparticles with oleic acid. *Appl. Surf. Sci.* **2003**, *211*, 315–320. [[CrossRef](#)]
116. Li, C.-C.; Chang, M.-H. Colloidal stability of CuO nanoparticles in alkanes via oleate modifications. *Mater. Lett.* **2004**, *58*, 3903–3907. [[CrossRef](#)]
117. Ma, X.; Lee, N.-H.; Oh, H.-J.; Kim, J.-W.; Rhee, C.-K.; Park, K.-S.; Kim, S.-J. Surface modification and characterization of highly dispersed silica nanoparticles by a cationic surfactant. *Colloids Surf. Physicochem. Eng. Asp.* **2010**, *358*, 172–176. [[CrossRef](#)]
118. Chang, S.-J.; Liao, W.-S.; Ciou, C.-J.; Lee, J.-T.; Li, C.-C. An efficient approach to derive hydroxyl groups on the surface of barium titanate nanoparticles to improve its chemical modification ability. *J. Colloid Interface Sci.* **2009**, *329*, 300–305. [[CrossRef](#)]
119. Du, Y.; Yin, Z.; Zhu, J.; Huang, X.; Wu, X.-J.; Zeng, Z.; Yan, Q.; Zhang, H. A general method for the large-scale synthesis of uniform ultrathin metal sulphide nanocrystals. *Nat. Commun.* **2012**, *3*, 1177. [[CrossRef](#)]
120. Bruce, I.J.; Sen, T. Surface Modification of Magnetic Nanoparticles with Alkoxysilanes and Their Application in Magnetic Bioseparations. *Langmuir* **2005**, *21*, 7029–7035. [[CrossRef](#)]
121. Vandenberg, E.T.; Bertilsson, L.; Liedberg, B.; Uvdal, K.; Erlandsson, R.; Elwing, H.; Lundström, I. Structure of 3-aminopropyl triethoxy silane on silicon oxide. *J. Colloid Interface Sci.* **1991**, *147*, 103–118. [[CrossRef](#)]
122. White, L.D.; Tripp, C.P. Reaction of (3-Aminopropyl)dimethylethoxysilane with Amine Catalysts on Silica Surfaces. *J. Colloid Interface Sci.* **2000**, *232*, 400–407. [[CrossRef](#)]
123. Ge, J.; He, L.; Goebel, J.; Yin, Y. Assembly of Magnetically Tunable Photonic Crystals in Nonpolar Solvents. *J. Am. Chem. Soc.* **2009**, *131*, 3484–3486. [[CrossRef](#)]
124. Yu, B.; Qian, L.; Yu, J.; Zhou, Z. Effects of Tail Group and Chain Length on the Tribological Behaviors of Self-Assembled Dual-Layer Films in Atmosphere and in Vacuum. *Tribol. Lett.* **2009**, *34*, 1. [[CrossRef](#)]
125. Iijima, M.; Tsukada, M.; Kamiya, H. Effect of particle size on surface modification of silica nanoparticles by using silane coupling agents and their dispersion stability in methylethylketone. *J. Colloid Interface Sci.* **2007**, *307*, 418–424. [[CrossRef](#)]
126. Pham, K.N.; Fullston, D.; Sagoe-Crentsil, K. Surface Charge Modification of Nano-Sized Silica Colloid. *Aust. J. Chem.* **2007**, *60*, 662–666. [[CrossRef](#)]
127. Zeltner, M.; Grass, R.N.; Schaetz, A.; Bubenhofer, S.B.; Luechinger, N.A.; Stark, W.J. Stable dispersions of ferromagnetic carbon-coated metal nanoparticles: Preparation via surface initiated atom transfer radical polymerization. *J. Mater. Chem.* **2012**, *22*, 12064–12071. [[CrossRef](#)]
128. Zhao, B.; Zhu, L. Mixed Polymer Brush-Grafted Particles: A New Class of Environmentally Responsive Nanostructured Materials. *Macromolecules* **2009**, *42*, 9369–9383. [[CrossRef](#)]
129. Rodriguez, R.; Herrera, R.; Archer, L.A.; Giannelis, E.P. Nanoscale Ionic Materials. *Adv. Mater.* **2008**, *20*, 4353–4358. [[CrossRef](#)]
130. Mallakpour, S.; Madani, M. A review of current coupling agents for modification of metal oxide nanoparticles. *Prog. Org. Coat.* **2015**, *86*, 194–207. [[CrossRef](#)]
131. Shaw, D.J. *Introduction to Colloid and Surface Chemistry*, 4th ed.; Butterworth-Heinemann: Oxford, UK; Boston, MA, USA, 1992.
132. Russel, W.B.; Russel, W.B.; Saville, D.A.; Schowalter, W.R. *Colloidal Dispersions*; Cambridge University Press: Cambridge, UK, 1991.
133. Van Der Hoeven, P.C.; Lyklema, J. Electrostatic stabilization in non-aqueous media. *Adv. Colloid Interface Sci.* **1992**, *42*, 205–277. [[CrossRef](#)]
134. Rubio-Hernández, F.J. Is DLVO Theory Valid for Non-Aqueous Suspensions? *J. Non-Equilib. Thermodyn.* **2005**, *24*, 75–79. [[CrossRef](#)]
135. Briscoe, W.H.; Horn, R.G. Direct Measurement of Surface Forces Due to Charging of Solids Immersed in a Nonpolar Liquid. *Langmuir* **2002**, *18*, 3945–3956. [[CrossRef](#)]
136. Carey, A.A. The Dielectric Constant of Lubrication Oils, n.d.:9. Available online: www.dtic.mil/docs/citations/ADA347479 (accessed on 10 August 2018).
137. Napper, D.H. Steric stabilization. *J. Colloid Interface Sci.* **1977**, *58*, 390–407. [[CrossRef](#)]

138. Smitham, J.B.; Napper, D.H. Steric stabilization in worse than θ -solvents. *Colloid Polym. Sci.* **1979**, *257*, 748–756. [[CrossRef](#)]
139. Zhulina, E.B.; Borisov, O.V.; Priamitsyn, V.A. Theory of steric stabilization of colloid dispersions by grafted polymers. *J. Colloid Interface Sci.* **1990**, *137*, 495–511. [[CrossRef](#)]
140. Gerber, P.; Moore, M.A. Comments on the Theory of Steric Stabilization. *Macromolecules* **1977**, *10*, 476–481. [[CrossRef](#)]
141. Hamaker, H.C. The London—Van der Waals attraction between spherical particles. *Physica* **1937**, *4*, 1058–1072. [[CrossRef](#)]
142. Bergstr, L. Hamaker constants of inorganic materials. *Adv. Colloid Interface Sci.* **1997**, *70*, 125–169. [[CrossRef](#)]
143. Srivastava, S.N.; Haydon, D.A. Estimate of the Hamaker constant for paraffinic hydrocarbons in aqueous suspensions. *Trans. Faraday Soc.* **1964**, *60*, 971. [[CrossRef](#)]
144. Vial, J.; Carré, A. Calculation of Hamaker constant and surface energy of polymers by a simple group contribution method. *Int. J. Adhes. Adhes.* **1991**, *11*, 140–143. [[CrossRef](#)]
145. Croucher, M.D.; Hair, M.L. Hamaker constants and the principle of corresponding states. *J. Phys. Chem.* **1977**, *81*, 1631–1636. [[CrossRef](#)]
146. Visser, J. On Hamaker constants: A comparison between Hamaker constants and Lifshitz-van der Waals constants. *Adv. Colloid Interface Sci.* **1972**, *3*, 331–363. [[CrossRef](#)]
147. Pinchuk, A.O. Size-Dependent Hamaker Constant for Silver Nanoparticles. *J. Phys. Chem. C* **2012**, *116*, 20099–20102. [[CrossRef](#)]
148. Jiang, K.; Pinchuk, P. Temperature and size-dependent Hamaker constants for metal nanoparticles. *Nanotechnology* **2016**, *27*, 345710. [[CrossRef](#)]
149. Yang, K.; Peng, H.; Wen, Y.; Li, N. Re-examination of characteristic FTIR spectrum of secondary layer in bilayer oleic acid-coated Fe₃O₄ nanoparticles. *Appl. Surf. Sci.* **2010**, *256*, 3093–3097. [[CrossRef](#)]
150. Kataby, G.; Cojocaru, M.; Prozorov, R.; Gedanken, A. Coating Carboxylic Acids on Amorphous Iron Nanoparticles. *Langmuir* **1999**, *15*, 1703–1708. [[CrossRef](#)]
151. Gun'ko, V.M.; Voronin, E.F.; Pakhlov, E.M.; Zarko, V.I.; Turov, V.V.; Guzenko, N.V.; Lebod, R.; Chibowski, E. Features of fumed silica coverage with silanes having three or two groups reacting with the surface. *Colloids Surf. Physicochem. Eng. Asp.* **2000**, *166*, 187–201. [[CrossRef](#)]
152. Ishida, H.; Koenig, J.L. Fourier transform infrared spectroscopic study of the structure of silane coupling agent on E-glass fiber. *J. Colloid Interface Sci.* **1978**, *64*, 565–576. [[CrossRef](#)]
153. Murat, M.; Grest, G.S. Structure of a grafted polymer brush: A molecular dynamics simulation. *Macromolecules* **1989**, *22*, 4054–4059. [[CrossRef](#)]



© 2019 by the authors. Licensee MDPI, Basel, Switzerland. This article is an open access article distributed under the terms and conditions of the Creative Commons Attribution (CC BY) license (<http://creativecommons.org/licenses/by/4.0/>).